ORIGINAL PAPER

APPLIED THERMODYNAMIC ANALYSIS IN SOLAR THERMAL SYSTEMS PERFORMANCE ASSESSMENT

ANDREEA-MIHAELA LET[1], VIVIANA FILIP[1], IOAN ALIN BUCURICA[2], SIMONA MIHAI[2], DORIN DACIAN LET[2]

Manuscript received: 08.01.2024; Accepted paper: 14.05.2024; Published online: 30.06.2024.

Abstract. *This paper presents the results of thermodynamic analysis applied to flat plate solar panels, incorporating both simulation studies and real system measurements in comparison. As solar thermal panels play a crucial role in sustainable energy solutions, analysis are essential for providing a detailed and accurate assessment of their performance. Thermodynamic tools like energy and exergy analyses can be used to evaluate and enhance the performance of solar thermal generation systems. Their usage can help identify the components and processes with the greatest potential for improvement, mainly in the design or exploitation phase. Exergetic analysis, in particular, reveals the true extent of losses, as demonstrated by energy and exergy analyses of various thermal power plants with different capacities. Exergy analysis provides a more accurate performance evaluation and is a valuable method for assessing and comparing potential configurations of these systems.*

Keywords: *solar thermal; thermodynamics; performance analysis.*

1. INTRODUCTION

Applied thermodynamic analysis of Solar Thermal Systems (STS) leverages energy and exergy analyses as robust tools for evaluating performance. These methods are instrumental in assessing the efficiency and effectiveness of various solar thermal collectors, such as flat-plate, PV/T, parabolic trough, and parabolic dish systems. By quantifying energy transformations and maximizing exergy potential, researchers gain insights into optimizing system configurations and enhancing overall sustainability.

Exergy analysis has been extensively investigated across various types of solar collectors in academic literature. Flat-plate solar collectors have received the most attention, representing the predominant focus of research efforts [1-2]. The second most prominent area of study involves combined photovoltaic and thermal (PV/T) collectors, which have also garnered substantial interest [3-4]. Parabolic trough collectors, while studied to a lesser extent, still constitute a significant area of research, albeit about one-third of the volume dedicated to PV/T collectors [5]. Parabolic dish collectors, known for their high exergetic efficiency, have been thoroughly analyzed and optimized by numerous researchers [6-7]. Other types of collectors, such as compound parabolic collectors, evacuated tube collectors, heat pipe collectors, and cavity receivers, have received comparatively less attention in the literature [8-9].

[1] Valahia University of Targoviste, Doctoral School of Engineering Sciences, 130004 Targoviste, Romania. E-mail: andreea.let@valahia.ro; v_filip@yahoo.com.
[2] Valahia University of Targoviste, Institute of Multidisciplinary Research for Science and Technology, 130004 Targoviste, Romania. E-mail: ldorin@icstm.ro; bucurica_alin@icstm.ro; simona.mihai@valahia.ro.

https://doi.org/10.46939/J.Sci.Arts-24.2-c01

Definition: „Exergy is the amount of work obtainable when some matter is brought to a state of thermodynamic equilibrium with the common components of the natural surroundings by means of reversible processes, involving interaction only with the above-mentioned components of nature" [10]. The exergy measurement units are Joules [J] and rate in Watts [W]; the symbols used are B, Ex, X, and b, ex, x. It was also called "Availability" by Keenan [11] or "Available Energy" (Ω^R) by Gyftopoulos and Beretta [12].

Thermodynamics of STS can be analysed based on Keenan's interpretation: "The First Law states that in every cyclic process, either work is converted into heat or heat is converted into work. In this sense, it makes no distinction between work and heat except to indicate a means of measuring each in terms of equivalent units. Once this technique of measurement is established, work and heat become entirely equivalent for all applications of the First Law. The Second Law, on the other hand, marks the distinction between these two quantities by stating that heat from a single source whose temperature is uniform cannot be completely converted into work in any cyclic process, whereas work from a single source can always be completely converted into heat." [11].

Thermodynamic analysis typically involves distinguishing systems into closed loop and open loop categories (Fig. 1). Both types of systems have boundary conditions: energy (E) exchanges include work (W) and heat (Q) interactions. Generally, heat transferred into the system and work transferred out of the system are considered positive. One can express this, according to the first law of thermodynamics, for any process occurring between two states (1 and 2) that are in equilibrium:

$$\int_1^2 \delta Q - \int_1^2 \delta W = E_2 - E_1 \tag{1}$$

after integrations:

$$Q_{1,2} - W_{1,2} = E_2 - E_1 \tag{2}$$

Considering equation (2), one can observe that work and heat interactions are path-dependent, meaning their values vary based on the process pathway. In contrast, the energy change between states 1 and 2 is path-independent and determined solely by these states. The second law of thermodynamics, applied to the same system, can be formulated like:

$$\int_1^2 \frac{\delta Q}{T} \leq S_2 - S_1 \tag{3}$$

Thus, the entropy transfer between a closed system and its environment is dependant upon: the heat transfer across the boundary (δQ) and the boundary temperature (T). This entropy transfer distinguishes heat and work transfers as two forms of energy transfer. As equation (3) illustrates, only the energy transfer can induce entropy transfer. The entropy generated is expressed in equation (4):

$$S_{gen} = S_2 - S_1 - \int_1^2 \frac{\delta Q}{T} \geq 0 \tag{4}$$

In the context of STS, exergy denotes the maximum useful work attainable during a process that aligns the system with a heat reservoir, which is typically the environment. Shortly explained, exergy represents the energy available for practical purposes. When the

system and its surroundings achieve thermal equilibrium, exergy comes to zero. The maximum potential work, with constant specific heat c_p , is described by equation (5):

$$\dot{W}_{\max} = \dot{m}[(h - T_0 s)_{in} - (h - T_0 s)_{out}] = m\left[c_p(T_H - T_0) - T_0 \ln\frac{T_H}{T_0}\right] \quad (5)$$

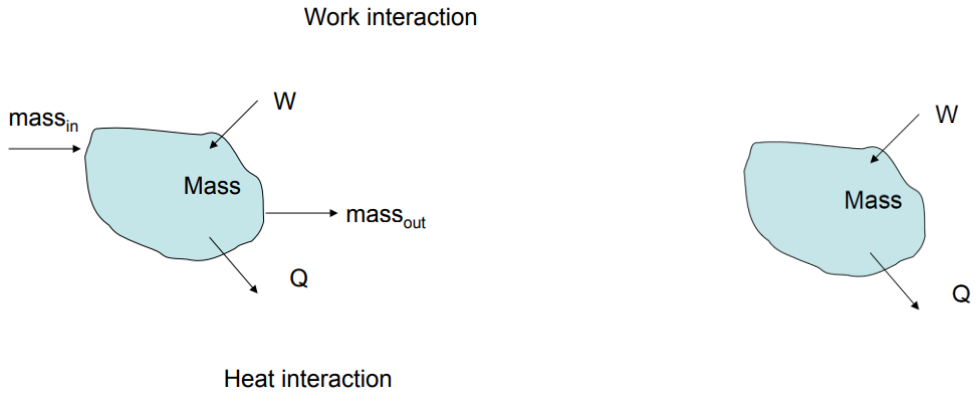

a) **b)**

Figure 1. Thermodynamics a) open system, b) closed system [13].

Exergy efficiency evaluates the efficiency of a process by incorporating the second law of thermodynamics. It measures how far a system deviates from a reversible state and is expressed as:

$$\eta_{II} = \frac{\dot{W}}{\dot{W}_{max}} = 1 - \frac{\dot{W}_{lost}}{\dot{W}_{max}} \quad (6)$$

then, the Gouy-Stodola theorem:

$$\dot{W}_{lost} = T_0 \dot{S}_{gen} \quad (7)$$

It is important not to confuse Equation (6) with the first-law efficiency, which for a heat engine operating between two heat reservoirs at T_H and T_L is expressed as:

$$\eta_I = \frac{W}{Q_H} = \eta_{II}(1 - \frac{T_L}{T_H}) = \eta_{II}\,\eta_{\text{carnot}} \quad (8)$$

Solar radiation represents the effort into a solar thermal energy system, which is harnessed and converted into useful energy. By applying exergy principles, researchers can quantify the efficiency of this conversion process, taking into account the irreversibilities and losses. This approach provides a comprehensive assessment of how effectively solar radiation is utilized, enabling the optimization of solar energy systems for maximum efficiency and sustainability. Based on Petela [14] exergy analysis of thermal radiation, the exergy factor is:

$$\Psi = 1 - \frac{4}{3}\frac{T_0}{T} + \frac{1}{3}\left(\frac{T_0}{T}\right)^4 \quad (9)$$

where T represents the temperatures of radiation reservoir and T_0 represents the temperatures of the environment.

2. MATERIALS AND METHODS

2.1. MATERIALS

The TESTBED [15] for the analysis used the experimental solar thermal platform (Fig. 2) installed at the Institute of Multidisciplinary Research for Science and Technology from Valahia University of Targoviste. Initial results from this installation integration with the buildings HVACR (Heating Ventilation Air Conditioning and Refrigeration) system were presented as Interreg Europe good practice scenario [16].

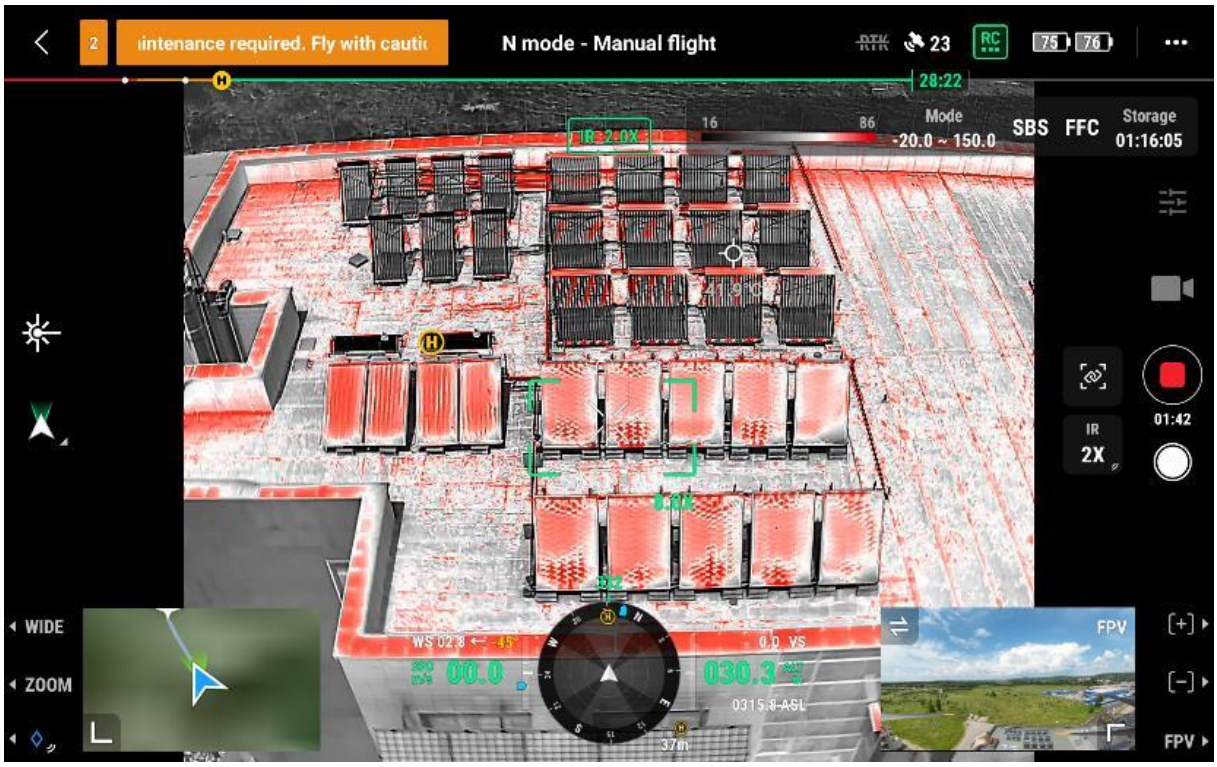

Figure 2. ICSTM solar thermal testbed (IR vision, thermography)

The ICSTM experimental platform was initially configured in 3 hydraulic circuits, each using its storage tank of 1000 liters individually connected to the HVACR building distribution system. Partially based on the work conducted in this paper, and financing from a national institutional funding project (CNFIS-FDI-2020-0397), the platform was modified for increased performance.

The new hydraulic scheme consists of circuit 1 (12 heat pipe colectors Westec SP-S58 configuration: 4series x 3paralel) and circuit 2 (14 plane colectors Tesy SP 07-250-ASL configuration 5s x 3p). Both solar arrays (approx. 20kW$_{th}$ installed) are being driven by solar pumping stations Taconova Circ ZR with Grunfos Solar PM2 high-efficiency pumps. Energy transfer from primary solar circuits is done through 2x puffer units of 500 liters each. This main energy transfer tanks are connected using a dedicated hydraulic transport circuit to a Thermal Energy Storage System TESS, which is comprised of 3 storage units Ferroli Ecounit 1000-2WB. The TESS can be used in 2 ways: directly (in cold seasons) connected to HVACR or indirectly using an energy conversion hot/cold performed through adsorption chiller SorTech eCoo 2.0 (2 units clustered for 32kW$_{th}$).

Measurement data is collected using a Resol Deltasol MX controller and datalogger system coupled with an extension module (due to large number of connected sensors and

controls). Datasets are stored locally with backup on FTP server at one minute resolution and in the manufacturers' cloud long-term storage servers with analysis features (Fig. 3). Some of the measurements were published as Open Data Sources in OpenAIRE - Zeonodo platform [17].

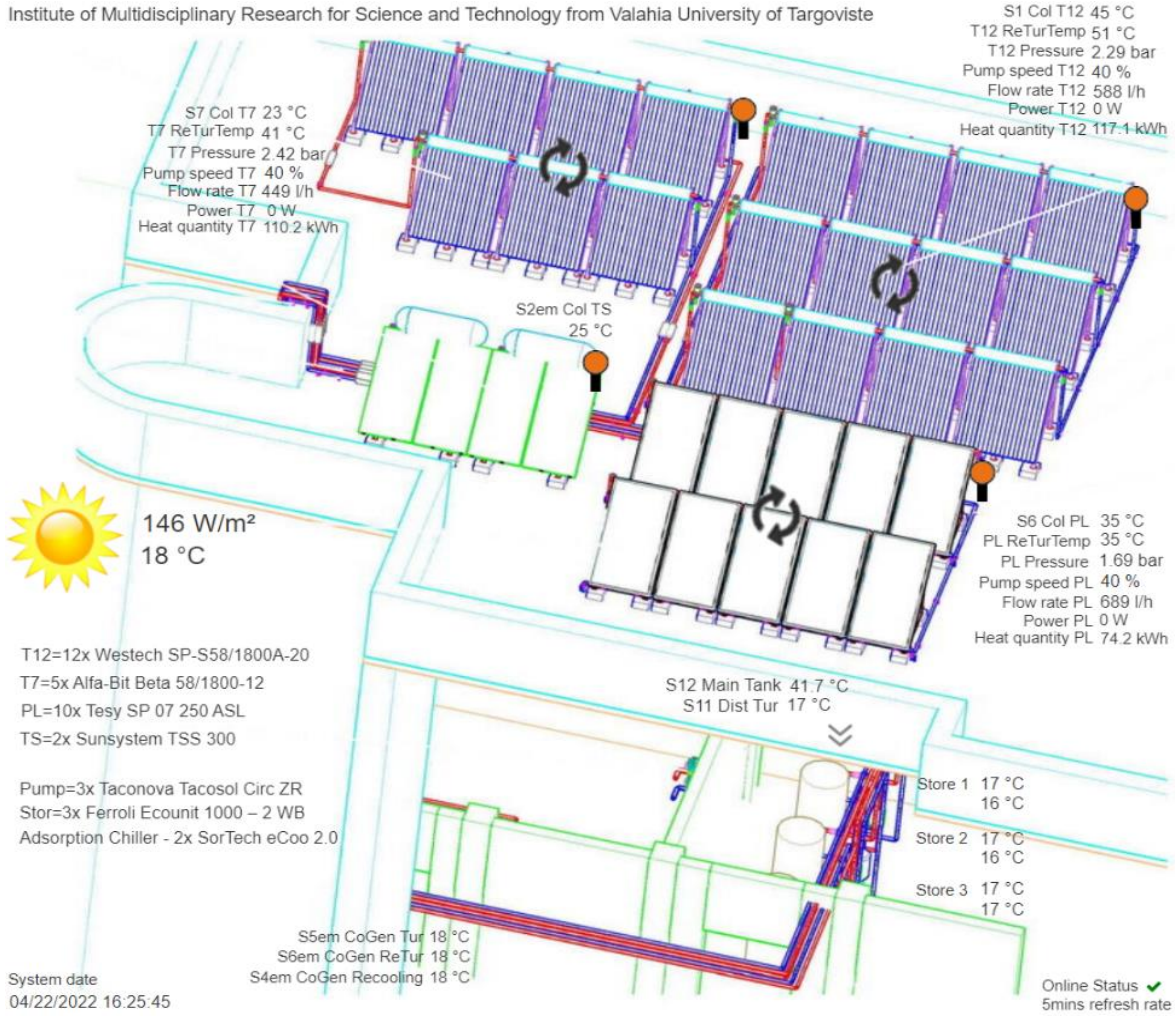

Figure 3. Measured data fields

Mathematical modeling and simulation of the testbed STS was performed in the T*SOL application developed by Valentin Software GmbH which is a company founded in 1988 that begun selling this product in 1993. T*SOL is a dynamic simulation program for the design, optimization and calculation of solar thermal systems. The application uses Meteonorm climate data by location database for the latest TMY data of the DWD. Locations not included are interpolated using satellite data and neighboring ground measuring stations.

2.2. METHODS

For conducting applied thermodynamic analysis in STS performance assessment, authors used simulated values (obtained from the modeling software) compared with measured ones (at times extrapolated values) to compute energy and exergy values. T*SOL simulation program was used to calculate the yield of a thermal solar system (Fig. 4). It was also exploited for optimally designing the newly planned STS, dimension storage, and collector arrays and determining the economic efficiency. The interpretation from T*SOL

website: "The dynamic annual simulation calculates temperatures and energies in time increments of one to six minutes. System parameters such as the efficiency and solar fraction are calculated from the simulation results. The optimization of STS depends on many parameters (the best possible combination of storage tanks, heat generators, and collector areas). As control also has a major impact on efficiency, one can precisely set control parameters such as switching temperatures and sensor heights." [18].

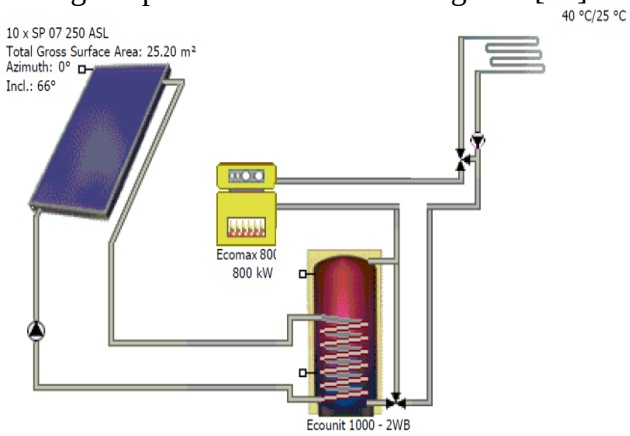

Figure 4. Solar thermal installation model

The measured values were analyzed from .csv files over a period of 6 years (from 2014) to identify the proper time intervals in which the system behaved as simulated in order to eliminate other functional behaviors. Datasets were pre-post processed in MS Excel. A typical data file contains 28 measured values at one-minute intervals; they are stored on SD card daily and over an FTP connection at monthly intervals. Missing data/data gaps were processed by generating Mean values depending on the total amount of lost data points.

Additional thermography measurements (Fig. 2) and sensors calibration verifications were conducted for data accuracy and thermal losses evaluation. Data deemed not credible was offset after sensor checks by 4 thermocouples calibrated measurement devices.

System losses were roughly estimated due to lack of information on thermal insulation and heat loses over the entirety of the outside and inside pipes length. The solar collector's losses were measured using a drone with high resolution IR camera. Handheld IR measurements were also conducted in tight inaccessible places. The overall conclusions of these evaluations were computed in the Excell data file, by adjusting computational formulas.

3. RESULTS AND DISCUSSION

In the following section, the parameters used in the mathematical model and results of the performed simulation, are presented (Tables 1-4, Fig. 5).

Table 1. Simulation Climate data

Location of Data Record	Targoviste City, Romania
Latitude N [°]	44.93
Longitude E [°]	25.43
Total Annual Global Radiation [kWh]	1335.1
Diffuse Radiation Percentage [%]	51.46
Mean Outside Temperature [°C]	9.55

Table 2. Collector loop connection

Volumetric Flow Rate [L/min]	15.87
Heat Transfer Medium: Water with Glycol [% : %]	60:40
Heat Capacity of Mixture [Ws/(kg K)]	3588

The collector loop pump control is dependent on the difference between the collector flow temperature and the tank reference temperature. The values used in the simulation are: switch on above a difference of 8°C and switch off below a difference of 3°C.

Table 3. STS Technical characteristics of circuit 2

Collector array		**Flat-plate collector specs.**	
Total Gross Surface Area	25.2 m²	Manufacturer:	Tesy LTD
Total Active Solar Surface	23.8 m²	Type:	SP 07 250 ASL
AreaNumber of Collectors:	10	Size:	
Installation:		Gross Surface Area:	2.52 m²
Tilt Angle:	66 °	Active Solar Surface:	2.38 m² (Aperture Area)
Azimuth Angle:	0 °	Heat capacity:	
Collector Surface Area Irradiation (Gross Surface):	33.31 MWh	Specific Heat Capacity:	5000 Ws/(m²K)
Piping:		Heat losses:	
Single (One-Way) Length of Piping System		Single Thermal Transmittance Coefficient:	3.56 W/(m²K)
Inside:	20 m	Quadratic Thermal Transmittance Coefficient:	0.0146 W/(m²K²)
Outside:	30 m	Optical losses:	
Between Collectors:	200 mm/Collector	Conversion Factor:	77.9 %
Heat Insulation Thermal Conductivity Coefficient Inside:	0.045 W/(m*K)	Incident Angle Modifier (IAM) for Diffuse Radiation:	87 %
Outside:	0.045 W/(m*K)	Incident Angle Modifier for Direct Irradiation for an Incident Angle of 50°:	92 %
Between Collectors:	0.045 W/(m*K)		
Nominal Diameter of Piping Inside and Outside:	28 mm		
Between Collectors: (Corresponds to a flow velocity of approx 0.5 m/s)	18 mm		
Thickness of Insulation Inside:	30 mm		
Outside:	30 mm		
Between Collectors:	20 mm		

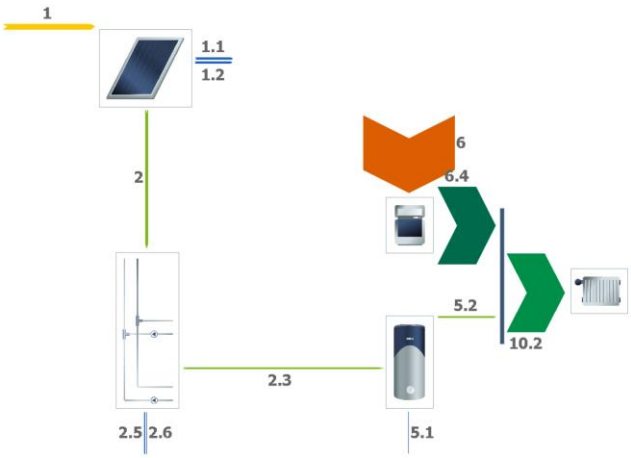

Figure 5. Energy balance of the system

Table 4. Simulation results

Fig. 5 index	**Parameter**	**Result**
1	Collector Surface Area Irradiation (Active Surface)	31.458 kWh
1.1	Optical Collector Losses	9.324 kWh
1.2	Thermal Collector Losses	9.696 kWh
2	Energy from Collector Array	12.438 kWh
2.3	Solar Energy to Buffer Tank	8.498 kWh
2.5	Internal Piping Losses	2.474 kWh
2.6	External Piping Losses	1.466 kWh
5.1	Buffer Tank Losses	923 kWh
5.2	Buffer Tank to Heating	7.569 kWh
6	Final Energy	562 MWh
6.4	Supplementary Energy to Space Heating	478 MWh
10.2	Heat to LT Heating	485 MWh

The simulation accounted for the fact that this solar thermal system is used as heat input for the HVACR system. This means that during cold seasons, the STS output is used directly for heating the fan coil units. The parameters of the simulation also considered the exact items (solar collectors, gas boilers, tank storage, etc.) used by the real system with their performance specifications. Consumption data was used as a total annual energy need designed for the building (7200 net usable space) and with a load profile computed from natural gas usage actually incurred (Zenodo dataset [17]). This approach was used due to lack of direct or indirect real measurement of the load.

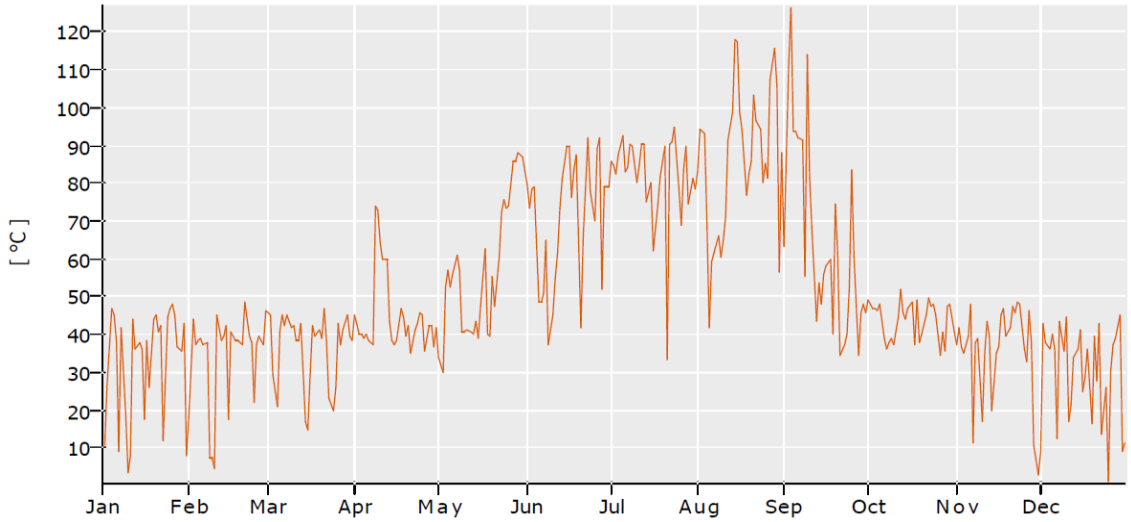

Figure 6. Daily maximum collector temperature (simulation results)

Fig. 6 represents the simulation results of the collector array annual temperature based on the initial hydraulic configuration. This was used as a reference and comparatively analyzed with previous measured values. During the months of August and September, one can observe temperatures over the water's boiling point. The stagnation temperature for these particular flat plate collectors is 110 degrees for glycol mixtures; thus, the system is at its maximum. This is due to the maximum head of the solar pump being used. To avoid this condition, the new hydraulic scheme reduces the pump head by 12 meters. The pumping stations were moved from the building's basement to the second floor right below the solar collector array.

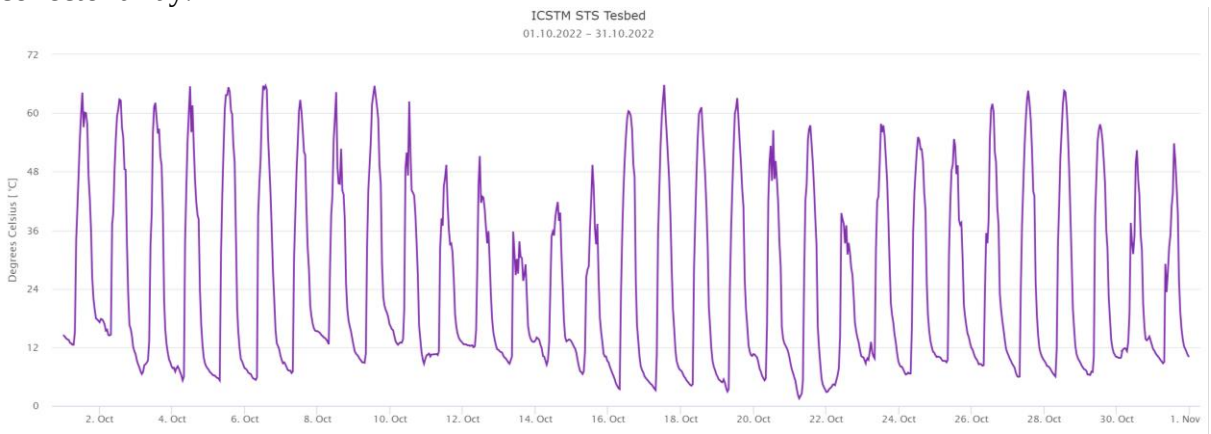

Figure 7. Measured monthly collector temperature

Comparing Fig. 7 with Fig. 6 for the same interval – month October, 2022 – one can observe average values of 12-50°C between the measured data and the simulation results of 35-50°C. This is due to the data display resolution of Fig. 6, but the maximum values are

important in this comparison (the minimum values depend on ambient temperature). This comment is used to validate simulation data.

The simulation performed took into account the 66 degrees inclination (mounting position) of the collectors, and thus provided the yield of the STS based on the available solar irradiation (also calculated on the surface of the collectors). Data was obtained from the Meteonorm climate database (computed from adjacent data sources for the Targoviste location). Results can be observed in Fig. 8.

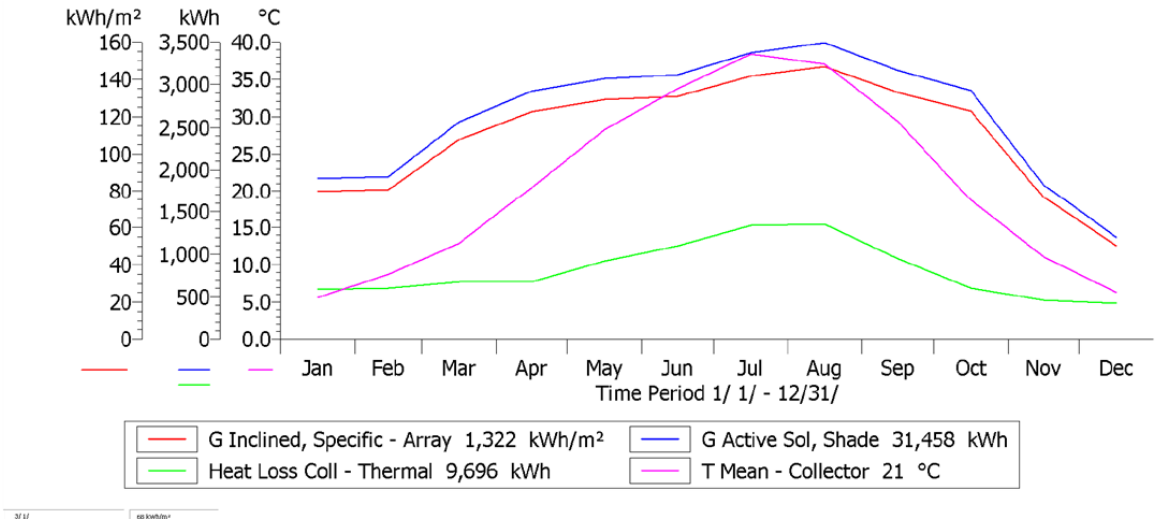

Figure 8. Collector array annual yield compared to available solar irradiation

Further study of the environmental impact on the STS performance helped in losses calculations. For this, the average ambient temperature, wind speed, and the length of pipes, diameters, and their insulation were computed. Fig. 9 presents the dependence of collector array temperature over the climatic parameters.

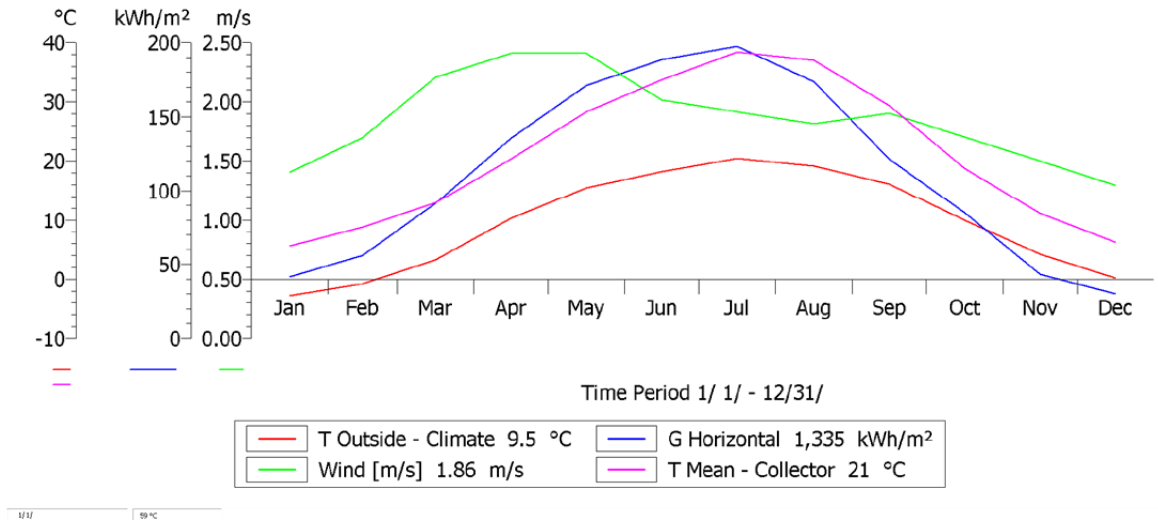

Figure 9. Collector array annual temperature compared to climatic conditions

For exemplifying the system operation based on real performance measurements, the following, are presented a couple of snapshots measured on the new system hydraulic scheme. The operating conditions for the study are cold but not too harsh a climate (typically late spring, or early autumn in Romania) with nighttime values over 10 degrees below comfort temperature. This forces rapid energy transfer through the building envelope, thus producing a need for additional energy input to keep indoor comfort temperatures.

The operating scenario studied is: STS-generated energy is transferred to primary puffer tanks; useful energy is stored in TESS which is then used for heating the return hydraulic circuit of the fan coil distribution system or the air handling units (depending on the amount of energy available). Conditioned by the outdoor temperature difference and the amount of stored heat inside the building, this scenario allows the operation of the HVACR system with STS as the primary heat source. When the temperature difference is higher, additional heating can be provided by a heat pump before engaging the gas boilers.

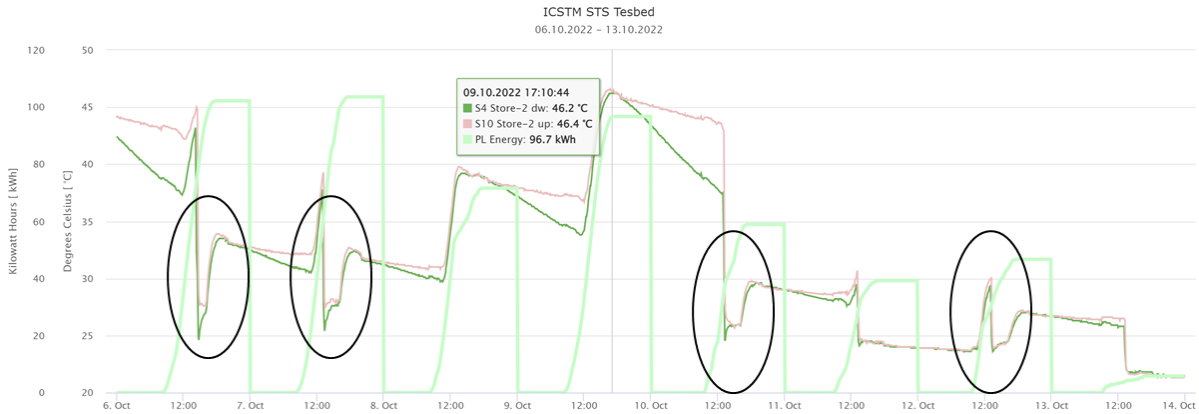

Figure 10. Studied scenario for one representative week

Fig. 10 represents a week containing the weekend days (8 and 9) in the middle. The graph shows the energy stored in TESS by the plane collectors through the primary puffer tanks. These indicate that there is no immediate effect of the energy produced by the solar array. The periods in which the air handling unit was used to discharge the TESS were encircled. The energy stored can be correlated with the TESS state of charge, and its recorded temperature, and because it's water storage tank the stratification phenomena count. For better observation of the storage tank entropy, both the upper-temperature sensor (S10) and the bottom one (S4) were plotted. The area between the two represents the energy not usable for work. The graph includes the energy value (in light green) of the plate collector's array. One can observe that over the weekend without consumption from TESS, the energy accumulated day-by-day was used on Monday's building's pre-heating stage.

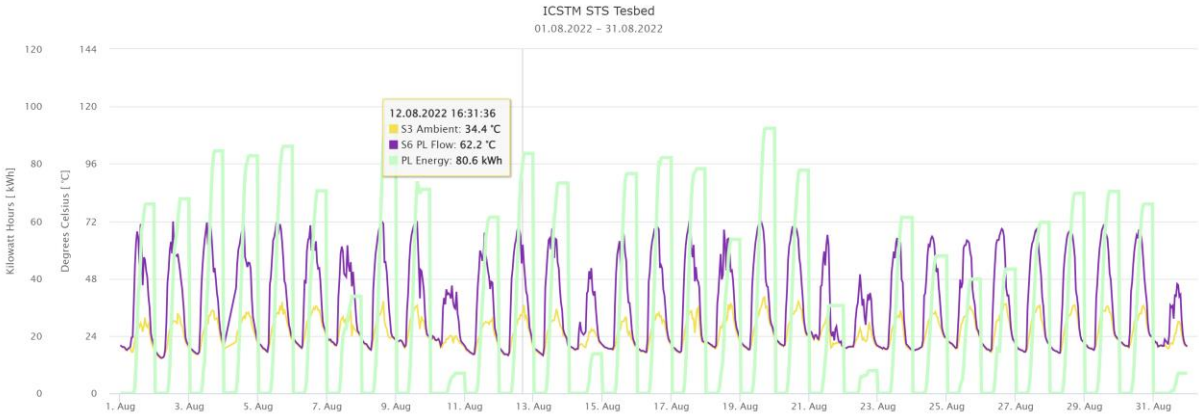

Figure 11. Monthly energy production

For a better understanding of the phenomena, it was selected the August month as being representative for the site's average local climatic conditions. In Fig. 11 the interdependence between collector temperature and energy produced by the array is overlapped with ambient temperature. Ambient conditions directly impact the conversion process effectiveness. Depending on the insulation performance of the collectors, more or less

energy is lost. IR thermography was used to verify the insulation of the solar collectors and one can observe from Fig. 2 that the heat-pipe collector type is better protected from thermal losses. Other STS losses were studied in terms of heat production, transport, and storage. The learnings were integrated into the model and thus the method was improved. Final observations of the study resume in the following:

Minimum Work = Exergy

$$W_{min} = \frac{\dot{W}_{rev}}{\dot{m}} = \Delta H - T_0 \Delta S = \left(H_{p,T} - H_{p_o,T_0}\right) - T_0 (S_{p,T} - S_{p_0,T_0})$$

$$B = (H - T_0 S) - (H - T_0 S)_0$$

$$W_{min} = \frac{\dot{W}_{rev}}{\dot{m}} = B_{out} - B_{in} \tag{10}$$

considering:

$$\dot{W} = \dot{B}_{out} - \dot{B}_{in} + T_o \dot{S}_{generated} \tag{11}$$

let

$$\dot{W} = \dot{W}_{min} + W_{lost} \tag{12}$$

then

$$\dot{W}_{lost} = \dot{B}_{lost} = T_0 \dot{S}_{generated} \tag{13}$$

were equation 13 expresses the Lost Work and thus, the Lost Exergy.

4. CONCLUSIONS

After identifying the primary STS losses and evaluating their impact over the system energy balance based on the simulation results, a decision to reconstruct the system was made. A new hydraulic scheme was designed to repose existing components. New primary energy exchange puffers were included in the schematic along with a new energy transport hydraulic system coupled with a rebuilt TESS. The STS rebuilt was carefully considered and evaluated due to financial constraints.

The paper presented the simulation results compared to real values of system performance measured after the works were completed. The information obtained during the computations was synthesized here to highlight the importance of energy and exergy analysis use in solar thermal systems. As it can be observed from the simulation results, STS in large buildings with high heat demands on an annual basis don't make economic sense. The energy output represents roughly 1% of the needs, and a scale-up STS is not possible due to limited installation space availability.

From this study we concluded that well-dimensioned STS could provide a high impact during specific periods and seasons, when high-capacity heat generators (heat pumps or boilers, which typically endow large buildings) operate to low under their capacity, thus being inefficient and wasting power.

One very important aspect in STS coupled with TESS is the system entropy; which for a closed thermodynamic system, it's a quantitative measure of the amount of thermal energy not available to do work. From our investigations we concluded that system entropy is lowest in the afternoon, thus making STS unusable during most of the working day. For this purpose, the use of STS in HVACR systems needs a special approach, considering day-after-day storage or readiness of storage before the pre-heating time scenarios. TESS installed in HVACR systems adds further energy efficiency by providing a large number of fan coil units with a pool of energy for timely consumption. Large heat sources will be less used (smaller energy consumption) in conjunction with renewable energy generators which could handle small energy demands.

Acknowledgements: *This work was supported by: the multidisciplinary team of researchers from ICSTM; Ministry of Education, Project CNFIS-FDI-2020-0397: Performanță și excelență în cercetarea multidisciplinară / Performance and excellence in multidisciplinary research (PerExcel); Ministry of Education, Project CNFIS-FDI-2021-0075: Calitate, performanță, excelență – fundamente pentru un mediu stimulativ și competitiv în activitatea de cercetare / Quality, performance, excellence – foundations for a stimulating and competitive research environment (ProResearch); European Commission, Project H2020 824388: Integrated multi-vector management system for Energy isLANDs (E-LAND).*

REFERENCES

[1] Omeiza, L.A., Abid, M., Dhanasekaran, A., Subramanian, Y., Raj, V., Kozak, K., Mamudu, U., Azad, A.K., *Journal of Engineering Research*, 2024. Available online https://doi.org/10.1016/j.jer.2023.09.011.
[2] Struckmann, F., *Project Report - Analysis of a Flat-plate Solar Collector*, MVK160 Heat and Mass Transport, 2008. Available online https://www.lth.se/fileadmin/ht/Kurser/MVK160/Project_08/Fabio.pdf
[3] Herrando, M., Wang, K., Huang, G., Otanicar, T., Mousa, O.B., Agathokleous, R.A., Ding, Y., Kalogirou, S., Ekins-Daukes, N., Taylor, R.A., Markides, C.N., *Progress in Energy and Combustion Science*, **97**, 101072, 2023.
[4] Aguilar-Jiménez, J.A., Hernández-Callejo, L., Alonso-Gómez, V.' Velázquez, N., López-Zavala, R., Acuña, A., Mariano-Hernández, D., *Solar Energy*, **212**, 191, 2020.
[5] Alamdari, P., Khatamifar, M., Lin, W., *Renewable and Sustainable Energy Reviews*, **199**, 114497, 2024.
[6] Hamada, M.A., Khalil, H., Abou Al-Sood, M.M., Sharshir, S.W., *Applied Thermal Engineering A*, **219**, 119450, 2023.
[7] Manikandan, G.K., Iniyan, S., Goic, R., *Applied Energy*, **235**, 1524, 2019.
[8] Patil, R.G., Panse, S.V., Joshi, J.B., Dalvi, V.H., *Energy*, **155**, 66, 2018.
[9] Pranesh, V., Velraj, R., Christopher, S., Kumaresan, V., *Solar Energy*, **187**, 293, 2019.
[10] Bilgen, S., *Acta Physico-Chimica Sinica*, **25**(8), 1645, 2009.
[11] Keenan, J.H., *British Journal of Applied Physics*, **2**, 183, 1951.
[12] Gyftopoulos, E.P., Beretta, G.P., *Thermodynamics: Foundations and Applications*, Macmillan Coll Div, London, 1991.
[13] Rathinavel, S., Senthil Kumar, S., Senthilkumar, T.S., Vignesh Kumar, V., Thermodynamics of Fluids in Motion. In Kumar, S.K., Radhakrishnan, N.S. (eds.), *Handbook of Research on Aspects and Applications of Incompressible and Compressible Aerodynamics*, pp. 158-184, IGI Global, Pennsylvania, 2022.
[14] Petela, R., Exergy analysis of solar radiation. In Enteria, N., Akbarzadeh, A. (eds.), *Solar Thermal Sciences and Engineering Applications*, CRC Press, Taylor & Francis Group, 2013.
[15] ERA-Net SES ICSTM Testbed. Available online https://www.eranet-smartenergysystems.eu/ll/150/ICSTM.html.
[16] Best practice of technology integration in Interreg Europe S3Unica project; "HVACR integrated Control System with weather compensation and Solar Thermal input"; 2020. Available online https://www.interregeurope.eu/good-practices/hvacr-integrated-control-system-with-weather-compensation-and-solar-thermal-input.
[17] Open Data Sources: University campus buildings electrical and thermal demand and generation; OpenAIRE - Zenodo 2022-11-28; DOI: 10.5281/zenodo.7371390; https://data.niaid.nih.gov/resources?id=zenodo_7371389.
[18] T*SOL website: https://online.tsol.de/en/.